Few-electron ground states of charge-tunable self-assembled quantum dots

B. T. Miller, W. Hansen,* S. Manus, R. J. Luyken, A. Lorke, and J. P. Kotthaus
Sektion Physik, LMU München, Geschwister-Scholl-Platz 1, 80539 München, Germany

S. Huant
LMCI-CNRS, 38042 Grenoble, France

G. Medeiros-Ribeiro† and P. M. Petroff
Materials Department and QUEST, University of California, Santa Barbara, California 93106
(Received 4 October 1996; revised manuscript received 20 March 1997)

The few-electron ground states of self-assembled InAs quantum dots are investigated using high-resolution capacitance spectroscopy in magnetic fields up to 23 T. The level structure reveals distinct shells which are labeled as *s*-, *p*-, and *d*-like according to their symmetry. Our measurements enable us to resolve the single-electron charging not only of the lowest (s) state with two electrons but also of the second lowest (p) state with four electrons as pronounced maxima in the capacitance spectra. Furthermore, two peaks at higher energy can be attributed to charging of the *d* shell with the first two electrons. We discuss the energy spectrum in terms of spatial quantization energy, Coulomb blockade, and many-particle effects. At around $B=15$ T we observe a magnetic-field-induced intermixing of the *p* and *d* shell. Additional fine structure in the capacitance spectra is observed and discussed both in terms of nearest-neighbor Coulomb interactions and monolayer fluctuations of the dot size. [S0163-1829(97)01835-3]

I. INTRODUCTION

Semiconductor quantum dots can be considered as artificial atoms. In fact, as in natural atoms, these small electronic systems have a discrete spectrum of energy levels. The confining potential of quantum dots, however, is different from the Coulomb potential of atoms. It arises from the interplay of band offsets and charges that surround the confined electrons. Using field effect devices it is possible to fabricate quantum dots with a voltage-tunable number of electrons. The few-electron ground states of such dots have been studied experimentally by several techniques such as single-electron capacitance spectroscopy[1] and single-electron tunneling.[2,3] Most studies have been performed on lithographically defined quantum dots with a lateral confinement length of about 100 nm.[1–4] For these systems, the energy for adding a single electron is usually dominated by Coulomb charging effects. For smaller dots, which can be directly grown by self-assembly,[5,6] the spatial quantization energy becomes more important. Furthermore, the artificial atoms discussed here are not exactly identical. Therefore the energy spectra of dot arrays may show the interplay between intrinsic effects of individual dots and properties of the dot ensemble.

Previous studies of capacitance spectroscopy on large-scale arrays of self-assembled InAs quantum dots have demonstrated the strong spatial quantization due to the small dot diameter of about 20 nm.[7] Recently the single-electron charging of the *s* shell was reported.[8,9] The goal of the studies presented here was to resolve *all* discrete many-electron ground states and to study the magnetic-field dependence of the *p* shell. A high-resolution capacitance technique[10] enables us to examine small dot ensembles. The number of dots is thereby drastically reduced as compared to prior experiments on self-assembled dots which averaged over more than 10^6 dots.[7–9] The results presented here are obtained on ensembles where the number of dots ranges from one thousand to several tens of thousand. Due to the reduced inhomogeneous broadening we observe the single-electron charging of the *p* and *d* shell in the capacitance spectra of such self-assembled quantum dots. We are able to determine the Coulomb blockade as a function of electron number per dot. A magnetic field *B* applied perpendicular to the plane of our oblate dots lifts the orbital degeneracy of the *p* shell. From the dispersion of the splitting we derive a transport effective mass which is distinctly different from the one obtained from spectroscopic studies. At $B=15$ T we observe a magnetic-field-induced crossover from a *p*- to a *d*-like ground state. All this information gives us a complete picture of the evolution of the ground-state energies of self-assembled dots with electron occupation and magnetic field allowing a quantitative comparison with theory. In addition to the quantized energy states of noninteracting dots the capacitance spectra exhibit a highly reproducible fine structure that reflects ensemble properties. Interdot interactions and monolayer fluctuations of the dot heights as possible causes for this additional structure are discussed.

II. EXPERIMENTAL DETAILS

The samples are grown by molecular-beam epitaxy, generating InAs dots in the Stranski-Krastanow growth mode.[5–9,11–14] The dots are embedded into a suitably designed MIS (metal-isolator-semiconductor)-type GaAs/AlAs heterostructure, as described in Refs. 7 and 8. Figure 1 shows the essential layer sequence and a sketch of the conduction-band edge. The layer sequence starting from the substrate is as follows: buffer consisting of an AlAs/GaAs superlattice

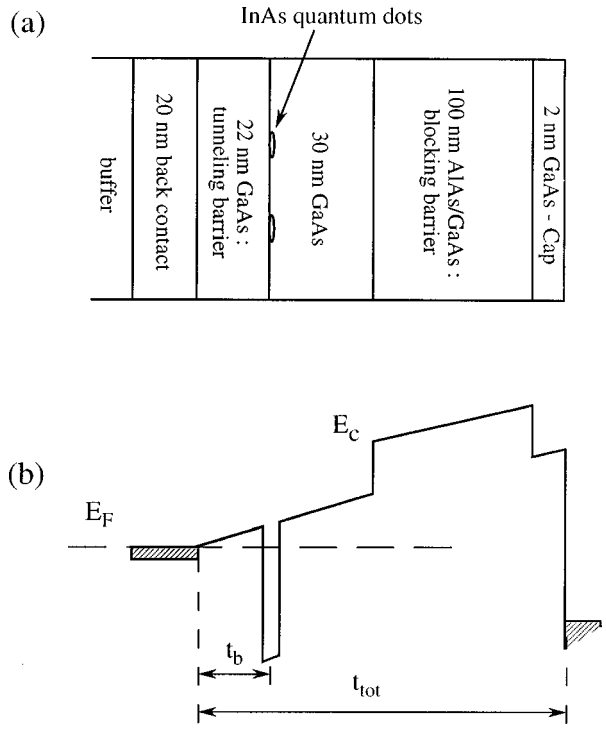

FIG. 1. (a) Layer sequence of our devices. The InAs dots are distributed within the plane sandwiched between two GaAs layers. (b) Sketch of the conduction-band edge E_c with respect to the Fermi level E_F along the growth direction for gate voltages at which no electrons are in the InAs dots. The indicated distances define the lever arm according to t_{tot}/t_b (in our case equal 7) which converts voltage into energy differences.

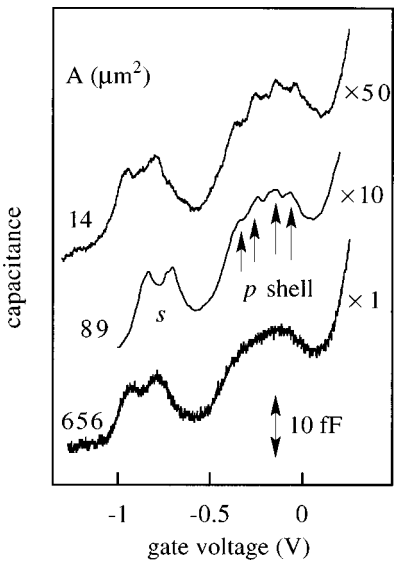

FIG. 2. Differential capacitance as a function of gate voltage recorded on samples with gate areas $A=14$, 89, and 656 μm^2 (from top to bottom) at $B=0$. The capacitance scale is given for the sample with $A=656$ μm^2 which has a total capacitance of 0.5 pF at $V_g=-1.2$ V. All other traces have been scaled by the indicated factors (within about 30% accuracy) and offset for clarity. Assuming a uniform density of 100 dots per μm^2 the different gate areas of the samples contain dot numbers from 1400 to 70 000. The amplitude and frequency of the excitation voltage are $dV=4$ mV and $f=170$ kHz, respectively. For the samples with $A=14$ and 89 μm^2 the single-electron charging of the p shell can clearly be resolved (denoted by the arrows for $A=89$ μm^2).

(period 4 nm); GaAs back contact layer, Si doped to 4×10^{18} cm^{-3}; GaAs tunnel barrier; the self-assembled quantum dots within the plane of an InAs wetting layer; undoped GaAs layer; blocking barrier consisting of an AlAs/GaAs superlattice (period 4 nm); GaAs cap layer. The dots are distributed within the plane of the wetting layer with a density in the range of 10^{10} cm^{-2}.[8] From atomic force micrographs of similarly grown samples we estimate the InAs dots to be approximately 20 nm in diameter and 7 nm in height.[5] They are remarkably uniform in size with their diameters and thicknesses fluctuating by only about 10%.[5,6] Ohmic contacts to the back contact are made with alloyed AuGe. On the crystal surface metal electrodes are defined by electron-beam lithography and thermal evaporation. The area A of this front gate determines the number of dots in the ensembles under investigation. Samples with $A=14$, 89, and 656 μm^2 were studied. The number of electrons per dot can be tuned with the bias applied between the gate and the back contact.

Measuring the capacitance-voltage (CV) characteristics of our devices allows us to study the electronic ground states of the dots. An increased capacitance signal with respect to the background reflects the gate voltage at which single electrons are injected into the dots. In a simple perturbative model of the N-electron ground-state energies the difference in gate voltage between two successive peaks is separated into terms for the electron-electron interaction and, whenever the two peaks are attributed to the filling of energetically different single-electron states, for the spatial quantization energy.[4,15]

The small capacitance of the self-assembled dot arrays is measured by a high-resolution capacitance bridge.[10] The technique is similar to the one applied by Ashoori *et al.*[1,16] The signal at the balance point is detected with a phase-sensitive amplifier via an on-chip impedance transformer. Voltage differences at the amplifier are proportional to capacitance values via a conversion factor containing the shunt capacitance of the balance point. The CV characteristics of the sample with the largest area $A=656$ μm^2 are measured using a more direct technique which yields current signals proportional to the absolute capacitance. The advantage and principal reason for the high resolution of the bridge measurements is the drastically reduced shunt capacitance and therefore noise level. In the measurements of the small-scale samples the noise level was reduced to about 20 nV at the balance point for a time constant of a few seconds enabling us to resolve capacitance changes as small as 4 aF. All measurements discussed below were performed at liquid-helium temperature ($T=4.2$ K) with an excitation amplitude of 4 mV and a frequency of 170 kHz.

III. RESULTS AND DISCUSSION

A. Quantized energy states of noninteracting dots

Figure 2 shows the CV traces of three samples with different gate areas recorded at $B=0$. The traces have been scaled by different multiplication factors and are offset for

clarity.[17] The samples are prepared from the same wafer, diced out of an area of about 20 mm^2. Assuming a uniform density of 100 dots per μm^2, the number of dots underneath the gates ranges from 1400 to 70 000. At low gate voltage, $V_g < -1.2$ V, the capacitive signal is determined by the parallel-plate capacitor formed by the back contact and front gate. The increase of the signal at large positive gate voltage, $V_g > 0.3$ V, reflects the charging of a two-dimensional electron gas in the InAs wetting layer. The well-resolved double structure at around $V_g = -0.8$ V arises from the charging of the dots with the first two electrons. We attribute these maxima to the *s* shell. We expect a fourfold degeneracy of the *p* shell, and thus four peaks at a higher gate voltage. In previous studies, however, the individual charging peaks of the *p* shell were not resolved due to inhomogeneous broadening in the dot ensemble investigated with mm^2 large gate areas.[7–9] Figure 2 shows that in our largest sample with $A = 656\ \mu m^2$ the broadening is still too strong for the four peaks of the *p* shell to be resolved. One broad shoulder around $V_g = -0.25$ V is observed. By decreasing the characteristic gate length below about 10 μm, inhomogeneous broadening due to long-range dot size variations is sufficiently reduced so that for the samples with $A = 89$ and 14 μm^2 the charging of the *p* shell with four individual electrons is observed.

The classification of the capacitance maxima according to the angular momenta of the shells is further confirmed by the magnetic-field dependence of the corresponding charging peaks. Figure 3(a) shows the CV traces of the sample with $A = 89\ \mu m^2$ for magnetic fields between 0 and 23 T, oriented perpendicular to the sample surface. The curves have been offset for clarity. The double structure of the *s* shell is only little affected by the magnetic field whereas the four maxima of the *p* shell exhibit a magnetic-field-dependent splitting, with two peaks decreasing with magnetic field and two increasing for $B < 15$ T. At small positive gate voltage two more peaks can be identified exhibiting a negative magnetic-field dependence for $B < 15$ T. We associate them to the charging of the *d* shell with the first two electrons. At around 15 T the magnetic-field dependence of the four highest observed maxima changes. Figure 3(b) displays the gate voltage positions of the dominant features against magnetic field as extracted from Fig. 3(a). To get a rough estimate for the corresponding energy scale we can divide the gate voltage differences by the lever arm (see Fig. 1). Screening of the gate potential by charges in the dots as well as by image charges is neglected in this approximation. The level structure is found to be atomlike with energy states comparable to shells. The many-electron ground states of self-assembled quantum dots are resolved as individual charging peaks for up to eight electrons in the dots.

Although deviations from a parabolic confining potential in our self-assembled dots have been observed,[9] we compare for the sake of simplicity the magnetic-field dependence of the data with the Fock model, i.e., a single-particle model which assumes a two-dimensional parabolic lateral confinement.[19] For $B = 0$ the energy-level diagram consists of equidistant energy states $E_{n,l} = (2n + |l| + 1)\hbar\omega_0$, where $\hbar\omega_0$ is the quantization energy and l is the angular quantum number, $l = 0, \pm 1, \pm 2, \ldots$ (for all states observed in our experiments the quantum number n is zero). The degeneracy of a state with energy $(m+1)\hbar\omega_0$ is $2(m+1)$ with $m = 2n + |l|$. As mentioned above we approximate the action of the electron-electron interaction by adding a corresponding term to the Fock states which lifts the degeneracy of the states. According to the quantum number l we have used the term *s* shell $(l = 0)$ for the double peak at large negative gate voltages, *p* shell $(l = \pm 1)$ for the four maxima at small negative gate voltages and *d* shell $(l = -2)$ for the two maxima at small positive gate voltage. Due to the charging of the wetting layer at $V_g > 0.3$ V, we are only able to observe two of the expected six *d* levels at high magnetic fields.

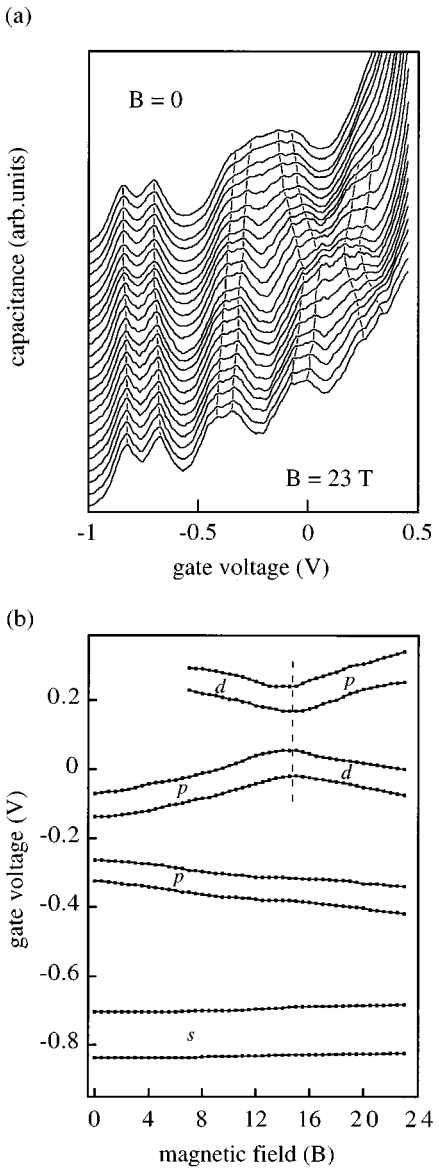

FIG. 3. (a) Differential capacitance of the sample with $A = 89\ \mu m^2$ at different magnetic fields applied in the growth direction. The traces are offset for clarity. From top to bottom the magnetic field is increased in steps of 1 T from $B = 0$ to 23 T. (b) Magnetic-field dependence of the individual charging peaks extracted from (a). The size of the symbols shows the accuracy for the determination of the peak positions which is about ± 5 mV.

As can be deduced from Figs. 3(a) and 3(b), the Coulomb charging energy depends on the number of electrons in the dots. At $B = 0$ we measure $\Delta V_g^{12} = 132$ mV for the two

maxima in the s shell and $\Delta V_g^{34}=61$ mV and $\Delta V_g^{56}=67$ mV for the first two and last two maxima in the p shell, respectively. The two peaks associated to the d shell can only be observed for $B>7$ T because of the strong increase of the capacitance in the corresponding gate voltage range due to the wetting layer. For $B=7$ T we get $\Delta V_g^{78}=65$ mV. The dependence of the Coulomb charging energy on the number of occupied states can be explained by the effective dot size which changes for different energy states according to the corresponding wave functions.[2,3] Our data show that the Coulomb charging energy of the present self-assembled quantum dots is drastically different for the s and p shell, whereas the difference between the p and d shell is negligible. The observed dependence of the Coulomb blockade on the number of electrons in the dots agrees well with a recent many-particle theory by Wojs and Hawrylak in which the few-electron ground states of similar self-assembled quantum dots is calculated.[20]

For the gate voltage difference between the states with two and three electrons in the p shell at $B=0$ we measure the large value of $\Delta V_g^{45}=128$ mV, which is nearly twice as large as ΔV_g^{34} and ΔV_g^{56}. The observation of the enhanced value for ΔV_g^{45} is corroborated by the strong curvature of the corresponding p levels for $B<2$ T, which can be observed in Fig. 3(b). Anisotropy of the dots may partly explain this observation.[21] An additional quantization term due to the anisotropy of the dots will increase ΔV_g^{45} with respect to ΔV_g^{34} and ΔV_g^{56}. Far-infrared (FIR) experiments on very similar dots show a splitting of the ω_+ and ω_- modes at $B=0$ which is explained by the anisotropy of the dots.[9] This splitting, however, amounts to about 2 meV corresponding to a gate voltage difference of only about 15 mV. Wojs and Hawrylak predicted that even for isotropic dots ΔV_g^{45} should be considerably larger than ΔV_g^{34} and ΔV_g^{56} due to an exchange-interaction term.[20] The filling of the dots with electrons should obey Hund's rules similar to the situation in atomic spectra. For a single lithographically defined quantum dot such a behavior has recently been observed in studies by single-electron tunneling.[3] Similarly, we attribute the large value of ΔV_g^{45} in our system predominantly to this exchange interaction.

With the gate voltage difference $\Delta V_g^{12}=132$ mV we can determine the s-shell charging energy of the isolated dot to be 21.5 meV where the lever arm as well as screening by the gates has been taken into account.[9,22] With this energy we estimate the characteristic length of the ground state l_0 and therefore the quantization energy $\hbar\omega_0$ to $l_0=5.3$ nm and $\hbar\omega_0=44$ meV.[23] These values nicely demonstrate that in our system the quantization energy is about a factor or two larger than the Coulomb charging energies. The values for the energies are in very good agreement with the ones obtained by capacitance and infrared transmission spectroscopy on large-scale dot arrays.[7,9]

We will now analyze in detail the magnetic-field dependence of the capacitance spectra. According to the theory of Fock the energy $E_{0,l}$ depends on magnetic field as

$$E_{0,l}=(|l|+1)\hbar\sqrt{(\omega_c/2)^2+\omega_0^2}+l\hbar\omega_c/2, \qquad (1)$$

where $\hbar\omega_c=\hbar eB/m^*$ is the cyclotron energy. The slight increase in gate voltage of the structure of the s shell ($l=0$) with magnetic field reflects the diamagnetic shift contained in the first term of $E_{0,l}$. The splitting of the two branches of the p shell ($l=\pm1$) is expected to be linear in magnetic field according to Eq. (1) with a slope yielding an effective mass of the electron system. For 2 T$<B<$13 T we observe a linear dependence and can thus extract an effective mass of $m^*=(0.057\pm0.007)m_e$. The change of the magnetic-field dependence of the highest four observed maxima at around $B=15$ T can only be explained by a change of the quantum numbers for the corresponding ground states. In fact, calculations of Wojs and Hawrylak confirm this statement.[20] They predict that a magnetic-field-induced intermixing of the p and d shell should occur at around $B=15$ T in remarkably good agreement with our observation. We can extract a gate voltage difference at the crossover point of $\Delta V_g^{67}=115$ mV. It should be mentioned that the Fock energy states—with $\hbar\omega_0=44$ meV and $m^*=0.057m_e$—describe the magnetic-field dependence of the experimentally determined capacitance maxima well within the accuracy of the measurements when the different single-electron states are offset by phenomenological energies corresponding to the Coulomb charging energies and the zero-field splitting of the two branches of the p shell (plot not shown here).

The effective mass of $m^*=(0.057\pm0.007)m_e$ as derived from the orbital splitting of the individual charging peaks of the p shell in capacitance measurements is distinctly different from the one obtained from spectroscopic studies. FIR experiments yield a value of $m^*=(0.082\pm0.008)m_e$ for a sample from the same wafer. The observation indicates that the Fock model is insufficient for a quantitative description of the experimental results. Considerable nonparabolic terms in the confinement potential might explain the discrepancy between the masses. On the other hand, in a parabolic potential where FIR experiments probe the bare effective mass—unaffected by electron-electron interactions—[24] in transport measurements electron-electron interactions contribute to the mass, resulting in a dressed mass.[25] For two-dimensional electron gases this effect is well known. Different values for the effective mass were observed for transport and spectroscopic experiments with the dressed mass being slightly larger than the bare one.[25] However, we observe the contrary for quantum dots where the transport mass is about 20% smaller than the FIR one. It is also important to note that both masses are considerably higher than the conduction-band edge mass of InAs, $m^*=0.023m_e$, and are closer to the one of GaAs, $m^*=0.067m_e$. This can be explained by the penetration of the dot wave function into the GaAs (Ref. 26) and additional effects of strain and nonparabolicity in k space.[9,27]

All of the discussion above reflects that we can quantitatively explain the dominant features in the measured capacitance spectra by the shell structure of the electron states in our artificial atoms assuming the dots to be equal and non-interacting. A more complex model involving the entire dot ensemble, however, is needed to explain small additional structure which can be observed in the CV spectra of the small area samples.

B. Ensemble properties

The gray scale plots in Figs. 4(a) and 4(b) depict the capacitance as a function of gate voltage and magnetic field

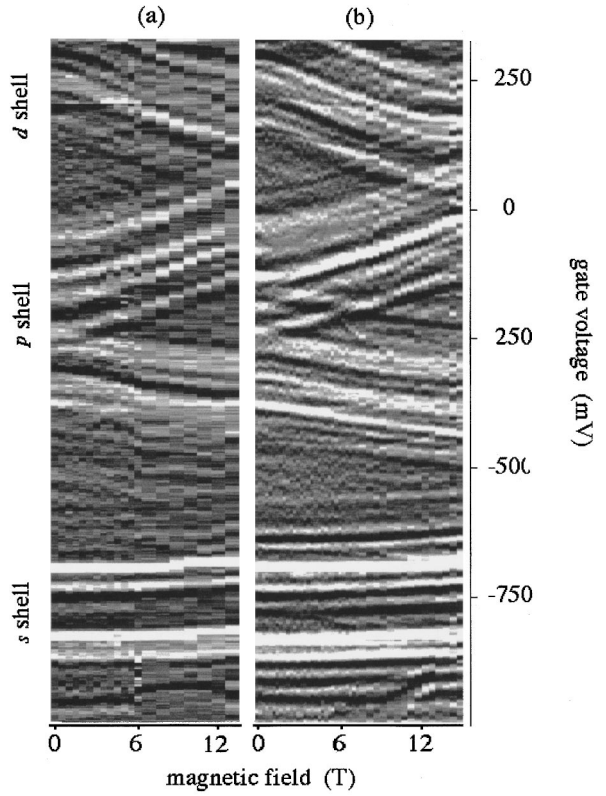

FIG. 4. Gray-scale plots of the capacitance of the same sample as in Fig. 3(a) for different thermal cycles. Data are recorded up to 13 and 14.5 T, respectively. The background of the raw data has been subtracted to obtain a better contrast. It can clearly be seen that the amplitude of the additional structure changes for different measurements, the energetic spacing between the replica, however, does not.

for the same sample as in Fig. 3(a). Between the measurements of Figs. 3(a), 4(a), and 4(b) the sample was thermally cycled. White areas in Fig. 4 correspond to maxima, black areas to minima in the capacitance. Here the background of the raw data is subtracted to obtain a better contrast. The additional maxima within the s, p, and d shells essentially show the same magnetic-field dependence as the dominant ones which, as shown above, correspond to the quantized energy states of noninteracting dots. A thorough investigation of the correlation between these peaks reveals that they can be grouped in sets. Each of these sets is essentially a replica of the spectrum of the main maxima shifted by roughly ± 40 mV [corresponding to approximately $\pm(5–6)$ meV] or multiples thereof with respect to the main spectrum.

Systematic measurements show that warming up and cooling down the sample changes the amplitude of this fine structure. The energetic spacing of the additional structure, however, is highly reproducible, even when different forward and reverse gate voltages are applied during the cooling procedure or when the cool down time is varied. Therefore the replica cannot be explained by a random background potential caused by frozen charges of the intentional or unintentional doping. One may, however, invoke fluctuations of the background charge in our samples to account for the change in the *amplitude* of the additional peaks with thermal cycling. The energetic fluctuations due to the background charge must be much smaller than the observed spacing of the replica.

One possible explanation for the systematically shifted spectra are monolayer fluctuations of the dot heights. Fluctuations where the height for different dots in the ensemble is assumed to vary uniformly by one or more monolayers will essentially result in a discrete offset of the threshold gate voltage. The lateral quantization energy will only be slightly affected. Numerical calculations of the ground-state energies of dots with different geometries support this argument.[28] An energy difference of approximately 6 meV is obtained for a monolayer change of the height assuming both lens-shaped dots and truncated pyramidal dots.

Another possible cause for the observed fine structure could be the nearest-neighbor interdot Coulomb interaction. Assuming clustering of dots an additional Coulomb energy will be necessary to charge a dot whose nearest-neighbor dot has already been charged. For an estimate of such an interdot interaction energy the nearest-neighbor distance of our dots has to be known. Recent results for similar self-assembled quantum dots indicate that this distance is typically twice the dot diameter and often much smaller than the average spacing between two dots as estimated from the dot density.[18,29,30] With such small nearest-neighbor distances interdot Coulomb interactions again yield energies comparable to the observed energy difference between the replica.

IV. CONCLUSION

In summary, we employ high-resolution capacitance spectroscopy to study the few-electron ground states of self-assembled quantum dots. We resolve Coulomb charging peaks in the p and d shell of the capacitance spectrum. We are therefore able to determine the Coulomb charging energy as a function of electron number per dot. A splitting of the states with two and three electrons in the p shell indicates the importance of the exchange energy similar to Hund's rule for atomic spectra. Furthermore, the orbital splitting of the p shell yields a transport effective mass of $m^*=(0.057 \pm 0.007)m_e$. This mass is significantly lower than the effective mass deduced from FIR spectroscopic studies. This might be explained by the nonparabolicity of the confinement potential or by many-particle effects that are known to result in different masses in high- and low-frequency transport studies. Experiments in high magnetic field up to 23 T show a magnetic-field-induced ground-state transition. The p shell and the d shell intermix at $B=15$ T. Below 15 T the fifth and sixth electrons are filled into p-like states which become d like for higher fields. The observed behavior is in very good agreement with model calculations. Additional fine structure is observed in the capacitance spectra of small dot ensembles and discussed in terms of ensemble properties such as interdot interactions and monolayer fluctuations of the dot heights.

ACKNOWLEDGMENTS

We would like to thank S. E. Ulloa, A. O. Govorov, D. Schmerek, and R. J. Warburton for continuous support as well as M. Grundmann, S. J. Allen, F. Simmel, and A. L. Efros for stimulating discussions. We would also like to

thank Dr. Ponse (Siemens AG, Munich) for supplying us with transistors. We gratefully acknowledge financial support by the DFG, BMBF, and the High Magnetic Field Laboratory, Grenoble. The work in Santa Barbara was funded by QUEST, a NSF Science and Technology Center. The collaboration between the LMU and QUEST is supported by an EC-US grant and by the Max Planck Society and the Alexander von Humboldt Foundation.

*Permanent address: Institut für Angewandte Physik, Universität Hamburg, Jungiusstr. 11, 20335 Hamburg, Germany.

†Permanent address: Hewlett-Packard Labs, 3500 Deer Creek Rd., Palo Alto, CA 94304.

[1] R. C. Ashoori, H. L. Stormer, J. S. Weiner, L. N. Pfeiffer, S. J. Pearton, K. W. Baldwin, and K. W. West, Phys. Rev. Lett. **71**, 613 (1993).

[2] T. Schmidt, M. Tewordt, R. H. Blick, R. J. Haug, D. Pfannkuche, K. v. Klitzing, A. Foerster, and H. Lueth, Phys. Rev. B **51**, 5570 (1995).

[3] S. Tarucha, D. G. Austing, T. Honda, R. J. van der Hage, and L. P. Kouwenhoven, Phys. Rev. Lett. **77**, 3613 (1996).

[4] M. Kastner, Phys. Today **46**(1), 24 (1993), and references therein.

[5] D. Leonard, M. Krishnamurthy, C. M. Reaves, S. P. Denbaars, and P. M. Petroff, Appl. Phys. Lett. **63**, 3203 (1993).

[6] J. M. Moison, F. Houzay, F. Barthe, L. Leprince, E. Andre, and O. Vatel, Appl. Phys. Lett. **64**, 196 (1994).

[7] H. Drexler, D. Leonard, W. Hansen, J. P. Kotthaus, and P. M. Petroff, Phys. Rev. Lett. **73**, 2252 (1994).

[8] G. Medeiros-Ribeiro, D. Leonard, and P. M. Petroff, Appl. Phys. Lett. **66**, 1767 (1995).

[9] M. Fricke, A. Lorke, J. P. Kotthaus, G. Medeiros-Ribeiro, and P. M. Petroff, Europhys. Lett. **36**, 197 (1996).

[10] D. Schmerek, S. Manus, A. O. Govorov, W. Hansen, J. P. Kotthaus, and M. Holland, Phys. Rev. B **54**, 13 816 (1996).

[11] L. Goldstein, F. Glas, J. Y. Marzin, M. N. Charasse, and G. Le Roux, Appl. Phys. Lett. **47**, 1099 (1985).

[12] Q. Xie, A. Madhukar, P. Chen, and N. P. Kobayashi, Phys. Rev. Lett. **75**, 2542 (1995).

[13] M. Grundmann *et al.*, Phys. Rev. Lett. **74**, 4043 (1995).

[14] J.-Y. Marzin, J.-M. Gerard, A. Izrael, D. Barrier, and G. Bastard, Phys. Rev. Lett. **73**, 716 (1994).

[15] C. W. J. Beenakker, Phys. Rev. B **44**, 1646 (1991).

[16] R. C. Ashoori, H. L. Stormer, J. S. Weiner, L. N. Pfeiffer, S. J. Pearton, K. W. Baldwin, and K. W. West, Phys. Rev. Lett. **68**, 3088 (1992).

[17] It can be seen for the sample with $A = 89\ \mu m^2$ that the gate voltage range for charging the dots with six electrons is smaller compared to the other samples. A similar small gate voltage range is observed for another large-scale sample prepared from a part of the wafer very close to $A = 89\ \mu m^2$ (not shown here). This reflects a slightly larger dot diameter as compared to the other samples and is caused by the intentional gradient of the In flux across the wafer (Refs. 8 and 18). A larger average dot diameter reduces the separation between the energy levels and therefore compresses the features in the capacitance spectrum.

[18] D. Leonard, K. Pond, and P. M. Petroff, Phys. Rev. B **50**, 11 687 (1994).

[19] V. Fock, Z. Phys. **47**, 446 (1928).

[20] A. Wojs and P. Hawrylak, Phys. Rev. B **53**, 10 841 (1996).

[21] C. Dahl, F. Brinkop, A. Wixforth, J. P. Kotthaus, M. Sundaram, and J. H. English, Solid State Commun. **80**, 673 (1991); S. K. Yip, Phys. Rev. B **43**, 1707 (1991).

[22] A. Lorke, M. Fricke, B. T. Miller, H. Haslinger, J. P. Kotthaus, G. Medeiros-Ribeiro, and P. M. Petroff, in *Proceedings of the 23rd International Symposium on Compound Semiconductors, St. Petersburg, 1996*, Inst. Phys. Conf. Ser. 155 (Institute of Physics and Physical Society, London, 1997), Chap. 11, pp. 803–808.

[23] U. Merkt, J. Huser, and M. Wagner, Phys. Rev. B **43**, 7320 (1991).

[24] Q. P. Li, K. Karrai, S. K. Yip, S. Das Sarma, and H. D. Drew, Phys. Rev. B **43**, 5154 (1991).

[25] J. P. Kotthaus, Surf. Sci. **73**, 472 (1978), and references therein.

[26] F. M. Peeters and V. Schweigert, Phys. Rev. B **53**, 1468 (1996).

[27] C. Gauer *et al.*, Semicond. Sci. Technol. **9**, 1580 (1994), and references therein.

[28] M. Grundmann (private communication).

[29] F. Heinrichsdorff, A. Krost, M. Grundmann, D. Bimberg, A. Kosogov, and P. Werner, Appl. Phys. Lett. **68**, 3284 (1996).

[30] N. P. Kobayashi, T. R. Ramachandran, P. Chen, and A. Madhukar, Appl. Phys. Lett. **68**, 3299 (1996).